Title	Effects of hollow structures added by selective laser sintering on the mechanical properties of Co-Cr alloy
Author(s) Alternative	Okano, H; Tasaka, A; Matsunaga, S; Kasahara, M; Wadachi, J; Hattori, M; Abe, S; Yamashita, S
Journal	Journal of prosthodontic research, 67(3): 460-467
URL	http://hdl.handle.net/10130/6258
Right	
Description	

J Prosthodont Res. 2023; 67(3): 460–467

OPEN ACCESS JPR Prosthodontic Research

Journal of Prosthodontic Research

Original article

Effects of hollow structures added by selective laser sintering on the mechanical properties of Co-Cr alloy

Haruna Okano [a], Akinori Tasaka [a], Satoru Matsunaga [b], Masaaki Kasahara [c], Juro Wadachi [a], Masayuki Hattori [c], Shinichi Abe [b], Shuichiro Yamashita [a,*]

[a] Department of Removable Partial Prosthodontics, Tokyo Dental College, Tokyo, Japan, [b] Department of Anatomy, Tokyo Dental College, Tokyo, Japan, [c] Department of Dental Materials Science, Tokyo Dental College, Tokyo, Japan

Abstract

Purpose: This study investigates the effects of hollow structures, added by selective laser sintering (SLS), on the mechanical properties of a Co-Cr alloy for providing an optimal structural property to the framework components of removable partial dentures (RPDs).

Methods: The specimens produced using the 3D data of the dumbbell-shaped cylinders were divided into four groups based on the manufacturing method: Cast, Mill, SLS-solid, and SLS-hollow. Tensile tests were performed to measure the mechanical properties of the specimens. The mechanical property values among the four groups were statistically compared using the Kruskal-Wallis test followed by the Steel-Dwass test ($\alpha = 0.05$).

Results: The median elastic modulus was the largest in the Cast, followed by SLS-solid, Mill, and SLS-hollow, with no significant differences observed between all conditions. The median ultimate tensile strength was the largest in the order of SLS-solid, Mill, SLS-hollow, and Cast. The median 0.2% proof stress was the largest in SLS-solid, followed by SLS-hollow, Cast, and Mill. The median elongation was the highest in the order of Mill, SLS-solid, SLS-hollow, and Cast.

Conclusions: With the addition of hollow structures, the elastic modulus decreased while the mechanical strength and proof stress remained high in SLS specimens. In addition, the ISO 22674 standard for dental metals was met, suggesting that SLS may be a possible method to design RPD frameworks with high strength and optimal structural properties.

Keywords: Inner structures, Selective laser sintering, Mechanical properties, Co-Cr alloy

Received 25 May 2022, Accepted 18 October 2022, Available online 19 November 2022

1. Introduction

With recent advances in 3D printer technology, selective laser sintering (SLS) has undergone rapid development, including the application to produce metal frameworks for removable partial dentures (RPD)[1–3]. Cobalt chromium (Co-Cr) alloys fabricated by SLS have excellent mechanical properties and fine homogeneous structures without precipitates, compared to those made by conventional casting or milling using computer numerical control (CNC) methods[4]. Clasps made by milling can prevent pattern deformation and casting shrinkage compared to conventional casting methods; however, they have limited fabrication accuracy owing to changes in the thickness of the burs used for cutting[5]. SLS has better fabrication accuracy, fatigue resistance, and mechanical properties[6]. This alloy has also been reported to have the mechanical properties of high tensile strength, yield strength, and elongation, which ensures a rigid metal framework and prevents the reduction in retention force caused by the permanent deformation of a clasp[7]. The occurrence of voids has been identified as a drawback of the casting method. However, voids can be minimized in SLS using localized heating and rapid solidification[8].

Unlike conventional sheet metal processing and machining, SLS technology enables adding complex shapes and inner structures to metals in the industrial field[9–12] for producing precision parts for aircraft and automobiles[13,14]. SLS directly molds an object from 3D CAD data; therefore, the inner structures of objects can be made hollow or mesh-type, reducing their weight. Furthermore, as SLS enables one-piece molding of complicated structures, it improves the strength of the connector region compared to the parts manufactured separately and then assembles by welding.

The inner lattice structures were added to the stem of an artificial femoral joint to obtain optimal mechanical properties similar to those of cortical bone in orthopedics. Consequently, the elastic modulus was successfully reduced to one-fifth of that of conventional implants[15]. SLS technology enables the addition of inner structures, unlike conventional processes, leading to localized changes in mechanical properties.

The required mechanical properties differ based on the metal framework components of RPD. For example, components such as the clasp, which uses undercuts, require elasticity[16–20], but the

DOI: https://doi.org/10.2186/jpr.JPR_D_22_00150
***Corresponding author:** Shuichiro Yamashita, Department of Removable Partial Prosthodontics, Tokyo Dental College, 2-9-18 Kandamisakicho Chiyoda-ku Tokyo, 101-0061, Japan.
E-mail address: syamashita@tdc.ac.jp

central part of the framework, such as the major connector, requires rigidity in a one-piece framework[18,21–24]. Mechanical properties required are adjusted by changing the width and thickness of the components in the conventional manufacturing method. The clasp requires a certain amount of elasticity. However, if an error occurs, harmful stress is produced on the abutment tooth during denture placement and removal[25]. Additionally, if a large connector lacks rigidity, uneven pressure is placed on the basal seat mucosa, increasing the risk of abutment tooth loss[24,26–28]. If the elastic modulus is controlled by the application of optimal micro-properties to the inner structure, elastic and rigid properties can be provided within a single framework. In implant-assisted RPDs (IARPD), the elastic modulus can be reduced by providing inner structures in the clasp arm and major connector that incorporate stress-breaking mechanisms. The pressure difference in the displacement of implants, abutment teeth, and the residual mucous membrane was appropriately managed by incorporating stress-breaking mechanisms in the major connector, which prevents overload on the implant body and local stress concentration in the framework. This method may lead to the possible manufacturing of RPDs where optimum elastic modulus can be achieved for each component instead of a uniform design. The retentive force, modeling accuracy, and fitting accuracy of clasps and frameworks made using SLS have been verified[29–31]; however, the mechanical properties of the inner structures remain unclarified.

This study investigates the effects of hollow structures, added by SLS, on the mechanical properties of Co-Cr alloys to provide an optimal structural property to the RPD framework components. The null hypothesis was as follows: the mechanical properties of the Co-Cr alloy were not affected by the addition of highly anisotropic structures inside the model shaped by SLS.

2. Materials and Methods

2.1. Specimen production

The test specimens were dumbbell-shaped cylinders consisting of holding and parallel sections. The outer shape was designed using 3D data design software (Geomagic Free Form,3D SYSTEMS, OR, USA) (outer shape stereolithography (STL) data). The size was based on ISO 22674:2016[32]. Each specimen was 59.0 mm long, and in the parallel section, the diameter and length were 3.0 mm and 18.0 mm, respectively (**Fig. 1**). The specimens were produced via casting (Cast), milling (Mill), or SLS. The SLS specimens were either solid (SLS-solid) or hollow inner structures (SLS-hollow). **Table 1** lists the materials used for each specimen and their elemental compositions. A wax disc (WAX DISKα, YAMAHACHI DENTAL MFG.CO., Aichi, Japan) was cut-processed from outer shape STL data using a cutting machine (DWX-51D, DGSHAPE Corporate, Shizuoka, Japan) to produce patterns for the cast specimens. The pattern was invested using a phosphate-bonded investment material (Remaexakt, Dentaurum GmbH & Co., Ispringen, Germany). Co-Cr alloy for casting (Remanium GM 800+, Dentaurum GmbH & Co., KG) and casting machine (Denko Auto sensor-MD-201 type, DKK Co., Ltd., Tokyo, Japan) were used to produce the specimen.

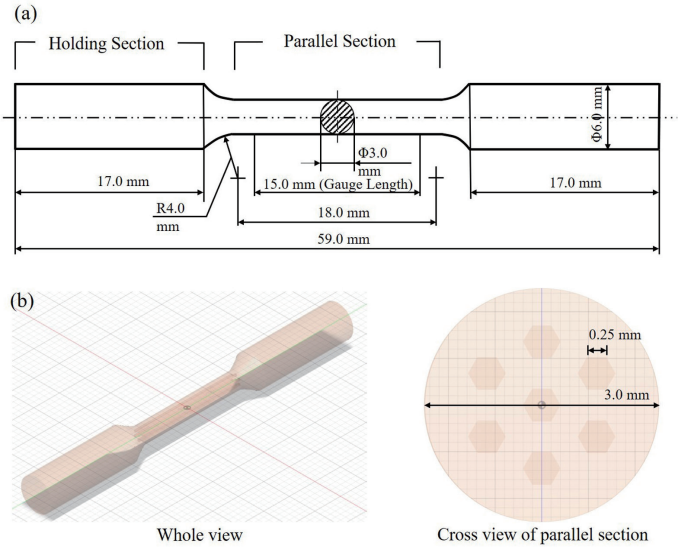

Fig. 1. (a) The schematic diagram and dimensions of specimen, (b) The design data of inner structure of SLS-hollow type specimen

Co-Cr alloy discs (KM-Cobalt Chrome CAD, KYOCERA Corporation, Kyoto, Japan) were milled from the outer shape STL data using a cutting machine (RPX500DSC, Roeders GmbH, Soltau, Germany) for Mill specimens. The processing conditions were as follows: spindle speed of 8500–25000 rpm, feed rate of 1300–2000mm/min, and a cutting depth of 0.05 to 0.30 mm.

SLS-solid specimens were additively manufactured using an SLS machine (EOSINT M270, EOS, Krailling, Germany) and Co-Cr alloy powder (SP2, EOS, Krailling, Germany). The laser power was 195.0 W, scan speed was 1200 mm/s, laser spot diameter was 0.1 mm, layering thickness was 0.02 mm, and modeling angle was 45.

SLS-hollow specimens were modeled using the 3D data design software (NETFABB, Autodesk, CA, USA). Hollow 0.25 mm hexagonal columns of 18.0 mm length along the parallel sections of the specimen were added as inner structures (**Fig. 1**). The hollow structure was determined by calculating the metal surface area required to achieve the same level of strength based on the percentage reduction in strength of specimens with internal mesh structures in the pilot study compared to that of solid specimens in tensile tests. The Co-Cr alloy powder, sintering machine, and molding parameters

Table 1. Manufacturing methods, brand names, manufactures, and elemental compositions of the four Co-Cr alloys tested

Manufacturing Method	Brand Name	Manufacturer	Elemental Composition(wt%)*								
			Co	Cr	W	Mo	Si	Fe	Mn	N	C
Cast	Remanium GM 800+	Dentaurum, Germany	58.3	32	1.5	6.5	1	N/A	<1.0	<1.0	<1.0
Mill	KM-Cobalt Chrome CAD	KYOCERA, Japan	61	28	8.5	N/A	≤4.0	N/A	≤4.0	≤4.0	N/A
SLS-solid SLS-hollow	SP2	EOS, Germany	65.8	25.7	5.9	5.6	1.2	≤0.5	≤0.1	N/A	N/A

* Provided by manufacturers. N/A: not available.

were the same as those used in SLS-solid. The specimens were modeled with residual powder in the hollow structure.

The same heat treatment was performed on SLS-solid and SLS-hollow as a finishing treatment. The temperature was raised from room temperature to 450 °C at 7.5 °C /min and held for 45 min and raised to 750 °C at 7.5 °C/min, held for 60 min, and then cooled in the furnace in an argon gas atmosphere after heat treatment. Subsequently, the support was removed. The specimens were sandblasted using Al_2O_3 powder (sand beads AW-S, ODEC, Osaka, Japan) under 0.75 MPa air-abrasion pressure with the metal surface processing machine (SAND BLAST FORTE, ODEC, Osaka, Japan).

The number of test specimens was 14 for each of the four groups, according to the ISO 22674 and the error permitted when shaping hollow structures.

2.2. Micro-CT observations of inner structures

The inner structures of specimens were observed using a micro-computed tomography (micro-CT) (XT H225 ST; Nikon, Tokyo, Japan). The imaging conditions were as follows. A voltage of 225 kV and a current of 155 μA. The images were analyzed using CT data analysis software (VG STUDIO, VOLUME GRAPHICS GmbH, Heidelberg, Germany) and an image processing software (ImageJ, National Institutes of Health, MD, USA)[33–35].

2.3. Measurement of mass and volume

The mass of specimens before the tensile test was measured using an electronic balance (HR-202i; A & D Company Limited, Tokyo, Japan). The volume was measured using a graduated cylinder (TPX (R); Sanplatec Corporation, Tokyo, Japan).

2.4. Measurement of mechanical property values

Tensile tests were performed at a 1.5 mm/min crosshead speed using a universal material testing machine (Autograph AG-20kNIS, Shimadzu, Kyoto, Japan) to measure mechanical properties. A load cell 20kN (SFL-20kNAG, Shimadzu, Kyoto, Japan) was to acquire the load signal, and the frequency was set to 50 Hz. The strain values were recorded using a video non-contact elongation meter (TRviewX 500D, Shimadzu, Kyoto, Japan). Tensile test results were used to calculate the elastic modulus, maximum tensile strength, 0.2% proof stress, and elongation.

2.5. Scanning electron microscopy (SEM) observations of microstructures

The fractured surfaces after testing were observed using an SEM (SU6600, Hitachi High Technologies Corporation, Tokyo, Japan). The acceleration voltage was set at 40 kV, and the measurement magnification was set at 1000×.

2.6. Statistical analysis

The mass, volume, and mechanical property values were statistically compared among the four groups: Cast, Mill, SLS-solid, and SLS-hollow. The Kruskal-Wallis test was performed. The Steel-Dwass test was used as the multiple comparison method because the Shapiro-Wilk test confirmed that the present study data did not follow the normal distribution. The significance level was set at 0.05. IBM SPSS Statistics version 21 (IBM, Armonk, NY, USA) was used for the Shapiro-Wilk and Kruskal-Wallis tests. The Statcel 4 software (OMS publishing Inc., Saitama, Japan) was used for the Steel-Dwass test.

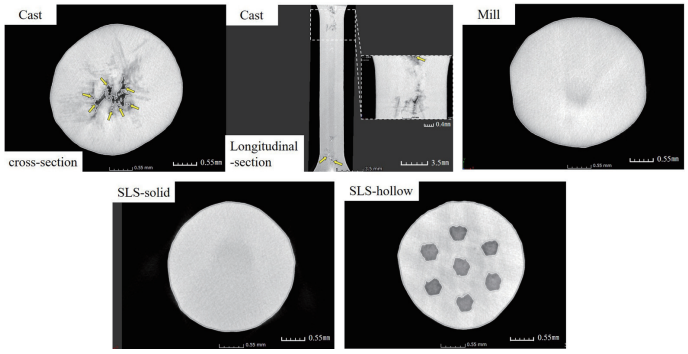

Fig. 2. Micro-CT image of specimens before tensile-test. Voids were observed only in the Cast specimens. The yellow arrows represent voids.

3. Results

3.1. Micro-CT observations of inner structures

Figure 2 shows a micro-CT image of specimens before tensile testing. Approximately, 10 voids with both width and height of 0.5 mm were observed at the boundary between the holding and parallel parts of cast specimens. No apparent voids were observed inside the Mill, SLS-solid, and SLS-hollow specimens. An inner hexagonal hollow structure was formed in SLS-hollow specimens with gray residual powder in it.

3.2. Mass/volume

Table 2 presents the median mass, volume, and interquartile range of the specimens of each group. The median mass was the largest in Mill (10.80 g), followed by Cast (10.15 g), SLS-solid (10.00 g), and SLS-hollow (9.90 g). Statistically significant differences were observed between all conditions except for Cast and SLS-solid (P <0.01, P <0.05) (**Fig. 3**). For median volumes, Cast (1.30 cm^3) and Mill (1.30 cm^3) as well as SLS-solid (1.20 cm^3) and SLS-hollow (1.20 cm^3) had the same values. The theoretical volume of SLS-hollow is 1.23 cm^3. There was a statistically significant difference between the SLS-solid and SLS-hollow for the cast as well as between SLS-solid and SLS-hollow for Mill (P <0.01) (**Fig. 4**).

3.3. Mechanical properties

Table 3 lists the mechanical properties of the Co-Cr alloy specimens in the four groups. **Figure 5** shows the stress-strain curve obtained from the tensile test. The median elastic modulus was the largest in Cast (180.9 GPa), followed by SLS-solid (178.2 GPa), Mill (163.4 GPa), and SLS-hollow (152.1 GPa) materials. No significant differences between conditions (P = 0.300) were observed (**Fig. 6**).

The median ultimate tensile strength was the highest in the order of SLS-solid (1355.5 MPa), Mill (1100.1 MPa), SLS-hollow (1083.5 MPa), and Cast (876.8 MPa). Statistically significant differences were observed between all groups except between Mill and SLS-hollow (P <0.01) (**Fig. 7**). The median 0.2% proof stress was largest in the SLS-solid (1204.7 MPa), followed by SLS-hollow (976.6 MPa), Cast (691.1

Table 2. Mass and volume of Cast, Mill, selective laser sintering (SLS)-solid, and SLS-hollow specimens. Each value is expressed as the median (interquartile range).

	Mass (g)	Volume (cm^3)
Cast	10.15 (0.20)	1.30 (0.05)
Mill	10.80 (0.50)	1.30 (0.01)
SLS-solid	10.00 (0.10)	1.20 (0.01)
SLS-hollow	9.90 (0.10)	1.20 (0.00)

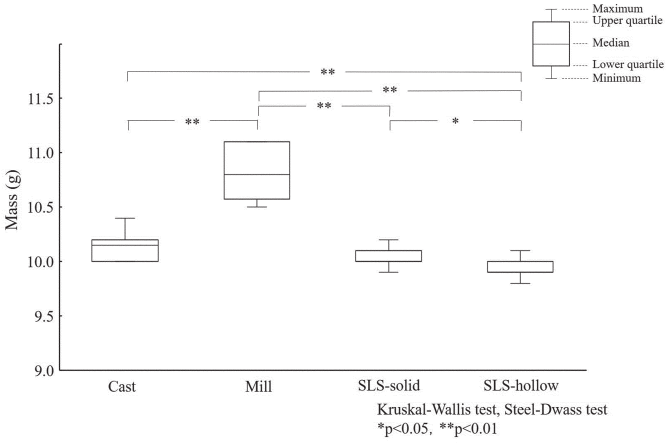

Fig. 3. Comparison of mass between Cast, Mill, SLS-solid, and SLS-hollow. Statistically significant differences were observed between all conditions except Cast and SLS-solid (P<0.01, P<0.05).

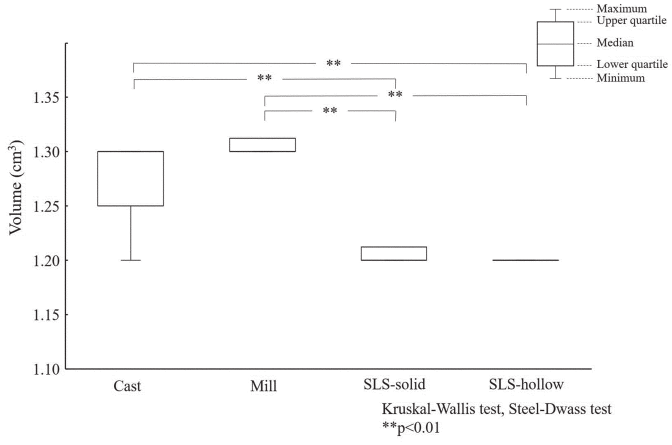

Fig. 4. Comparison of volume between Cast, Mill, SLS-solid, and SLS-hollow. There was a statistically significant difference between the SLS-solid and SLS-hollow for Cast, SLS-solid, and SLS-hollow for Mill (P<0.01).

Table 3. Mechanical properties of Cast, Mill, selective laser sintering (SLS)-solid, and SLS-hollow specimens after tensile testing. Each value is expressed as a median (interquartile range).

	Elastic modulus (GPa)	Ultimate tensile strength (MPa)	0.2% Proof stress (MPa)	Elongation (%)
Cast	180.9 (60.5)	876.8 (122.3)	691.1 (104.2)	2.5 (2.8)
Mill	163.4 (83.6)	1100.1 (56.0)	538.1 (44.8)	35.2 (7.7)
SLS-solid	178.2 (60.9)	1355.5 (31.4)	1204.7 (65.1)	4.1 (0.8)
SLS-hollow	152.1 (41.4)	1083.5 (39.1)	976.6 (71.2)	3.7 (1.2)

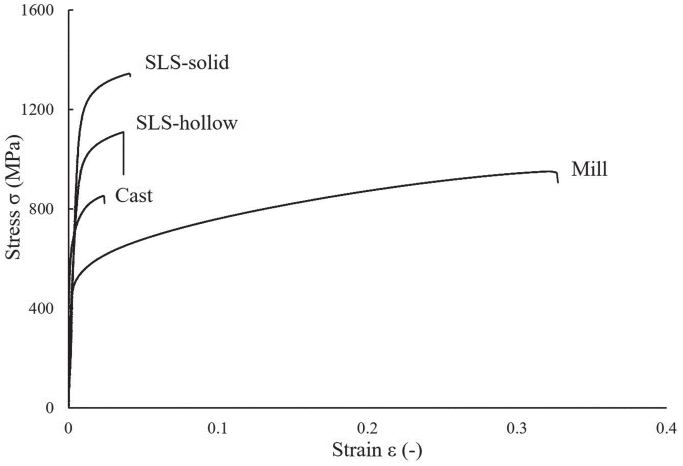

Fig. 5. Typical stress-strain curves of Cast, Mill, SLS-solid, and SLS-hollow

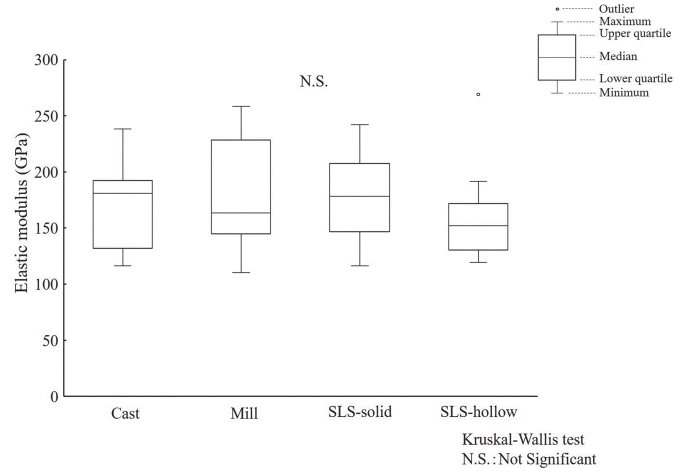

Fig. 6. Comparison of elastic modulus between Cast, Mill, SLS-solid, and SLS-hollow. No significant difference was observed between all the conditions (P=0.300).

MPa), and Mill (538.1 MPa). Statistically significant differences were observed between all groups (P <0.01) (**Fig. 8**).

The median elongation was highest in Mill (35.2%), followed by SLS-solid (4.1%). SLS-hollow (3.7%), and Cast (2.5%). Statistically significant differences were found between Cast and SLS-solid, as well as between Mill and the other three groups (P <0.01, P <0.05) (**Fig. 9**).

ISO 22674: 2016 (Dentistry—Metallic Materials for Fixed and Removable Restorations and Appliances) specifies the standard of mechanical properties of Type 5 materials with an elastic modulus of at least 150 GPa and a 0.2% proof stress of at least 500 MPa, and elongation of at least 2%[32]. In this study, these criteria were met in all four groups.

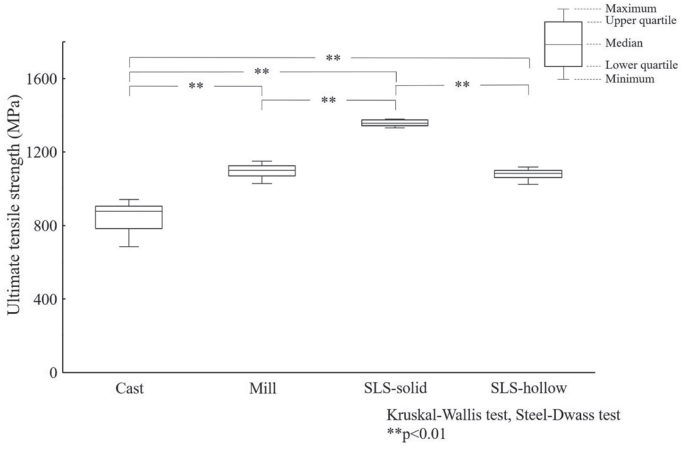

Fig. 7. Comparison of ultimate tensile strength between Cast, Mill, SLS-solid, and SLS-hollow. Statistically significant differences were observed between all groups except between Mill and SLS-hollow (P<0.01).

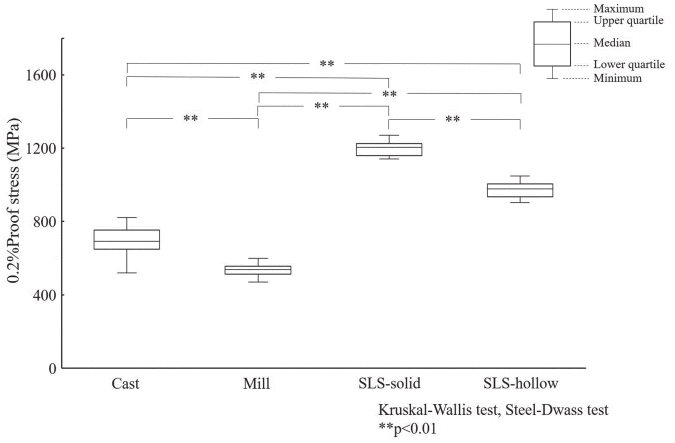

Fig. 8. Comparison of 0.2% Proof stress between Cast, Mill, SLS-solid, and SLS-hollow. Statistically significant differences were observed between all groups (P<0.01).

3.4. SEM observations of microstructures

Figure 10 shows SEM images of the fracture surfaces of the specimens after the tensile test. The fracture occurred along the border between the holding and parallel part where voids were observed in the micro-CT image of the Cast, middle of the parallel part for the Mill, and near the holding part of the parallel part on the tensile side for SLS-solid and SLS-hollow. The Cast specimens exhibited a relatively smooth fracture surface dotted with small voids, which are believed to be casting defects and wavy surfaces with cleavage (**Fig. 10**, cast). The Mill specimens showed a fracture surface with minor irregularities and fine dimples (**Fig. 10**; Mill). Smooth fracture surface and a cross-section fractured in a particular direction owing to the build-up of layers during the additive manufacturing and tear ridges were observed (**Fig. 10**; SLS-solid and SLS-hollow) for both SLS-solid and SLS-hollow. In addition to the characteristics observed in SLS-solid, crystal images of powder that was trapped and molded within the hollow structure may have fused during the SLS process with residual powder, which might have flowed out at the time of fracture, were observed in the SLS-hollow.

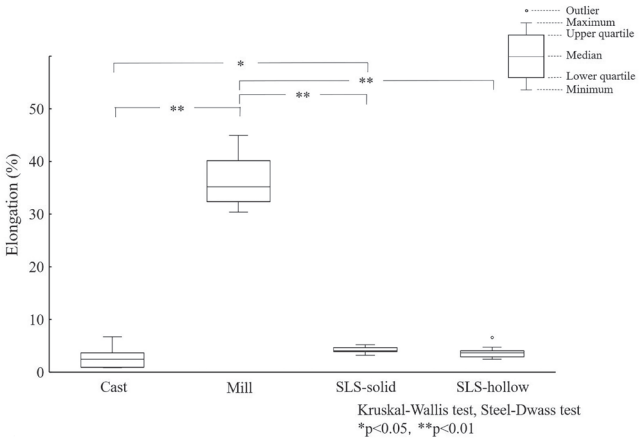

Fig. 9. Comparison of elongation between Cast, Mill, SLS-solid, and SLS-hollow. Statistically significant differences were found between Cast and SLS-solid as well as between Mill and the other three groups (P<0.01, P<0.05).

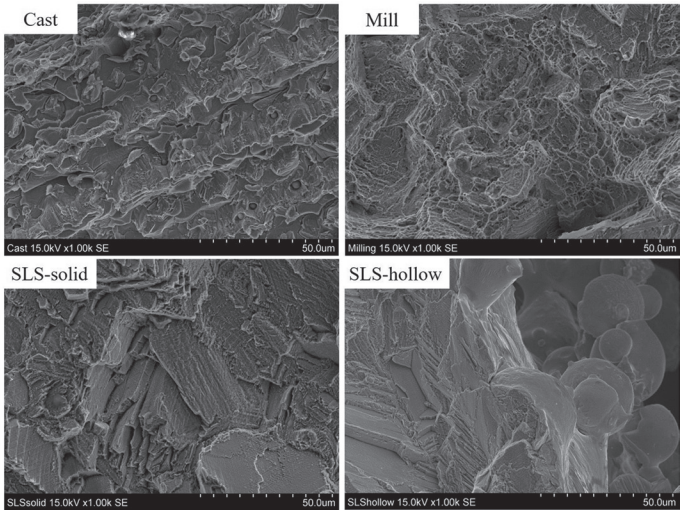

Fig. 10. SEM images of fracture surfaces of tensile-tested Cast, Mill, SLS-solid, and SLS-hollow specimens at 1000× magnification

4. Discussion

In this study, tensile tests were performed to verify whether the specimens with internal structure met the criteria for use as dental metals. Previous similar studies also used tensile tests to examine the mechanical properties of specimens produced by different fabrication methods. The SLS-hollow specimens with the hollow structures met the ISO standard 22674, suggesting that SLS technology is possible for clinical application.

There were no significant differences among the elastic modulus of the four groups. However, SLS-hollow had the smallest value, suggesting that the elastic modulus decreased with the addition of hollow structures.

The ultimate tensile strength and 0.2% proof stress values of SLS-solid were higher than those of the Cast and Mill, suggesting

that the SLS specimens had excellent mechanical strength and proof stress. When the SLS-hollow was compared to Cast and Mill, the ultimate tensile strength was close to that of Mill, but 0.2% proof stress was higher than that of Mill. However, these values were not as high as those of the SLS-solid, suggesting that SLS-hollow could achieve a certain mechanical strength and proof stress, although it is not equal to that of the SLS-solid. Residual powder in the material may have sustained the mechanical properties of the SLS-hollow even with the addition of hollow structures[36]. Further research is required on the effects of the residual powder on the mechanical properties of SLS specimens.

SLS-hollow and the SLS-solid displayed similar elongation and indicated no significant difference. Therefore, the presence or absence of hollow structures did not affect their ductility.

Although the chemical compositions of the Co-Cr alloys in the four groups were slightly different, as shown in **Table 1**, it was assumed that there was no effect on the mechanical properties[37].

Consequently, the null hypothesis that the mechanical properties of Co-Cr alloys remain unaffected by the addition of highly anisotropic structures inside the model shaped by SLS was partially rejected.

Voids and inner structures are believed to be significantly involved in the mechanical properties of the fabricated specimens. Voids are a significant disadvantage to the casting method. During a typical casting process, liquid metal is injected into the mold solidified from the outer surface. However, voids are formed owing to the shrinkage caused by the cooling and solidification of liquid metal[38,39]. Micro-computed tomography images before the tensile test and the fracture surfaces after the test showed non-uniform surfaces with voids in the Cast specimens. According to Mori *et al*., Casting Co-Cr alloys have low strength and ductility owing to their coarse microstructures and casting defects[40–42]. Voids, caused by shrinkage cavities, were found mainly at the boundary between the holding and parallel parts, where the diameter changed significantly from 3 to 6 mm[43]. Mill, SLS-solid, and SLS-hollow showed homogeneous and dense structures without voids. Specimens were cut from a metal disc for milling; therefore, the presence or absence of voids depends on the initial quality of the disc[44]. However, disc manufacturing is industrially controlled, and defects are rare. In SLS, the formation of defects and voids is minimized by rapid heating and cooling of the Co-Cr alloy powder[45]. The fracture site of the specimen in the tensile test was observed during void development in the Cast. The diameters of parallel sections of the specimens in each group were Cast (3.10 mm), Mill (3.10 mm), SLS-solid (3.02 mm), and SLS-hollow (3.01 mm). The diameters were measured at three points on the parallel sections in preliminary experiments; however, no clear relationship between the fracture site and the diameter of the specimen was obtained.

The SLS-solid showed a high ultimate tensile strength and 0.2% proof stress. The SLS method produces smaller crystal grains than casting[46]. The refined grains of the crystals contribute to excellent mechanical strength and proof stress[47,48]. The mechanical properties deteriorated due to the segregation of dendrite in Cast. However, the rapid solidification most likely increased the dissolution limit of solute elements, thus reducing the segregation of dendrites in SLS-solid[48].

The differences in structure inside the specimens were also observed from the SEM image of the fracture surface. The fracture surfaces of the Cast specimens showed cleavage and voids, which indicated typical brittle fracture behavior with poor ductility. The fracture surface of Mill specimens showed fibrous fracture surfaces and dimples, suggesting ductile fracture occurred due to the propagation of cracks from shearing and tearing.

The fracture surfaces of the SLS-solid and SLS-hollow were dense with no voids. In addition, some tearing ridges were observed, suggesting brittle fracture with plastic deformation.

Therefore, adding hollow structures similar to SLS-hollow could benefit an RPD framework due to its high strength and optimum structural properties. Furthermore, no voids were found in SLS specimens; therefore, specimens with consistent qualities would be provided compared to conventional casting. In addition, SLS-hollow showed a significantly smaller mass than all other groups, suggesting that the addition of inner structures is a possible way to reduce the weight of the framework.

The limitation of this study is that the residual powder in the inner hollow structures is not removed. Therefore, it is necessary to add holes to the SLS-hollow model to remove the residual powder before measuring the mechanical properties in the future. Furthermore, it is necessary to explore more patterns in the future to investigate the relationship between the elastic modulus and inner structures in SLS models as only one type of hollow structure is used in this study. Additionally, mechanical properties were investigated using specimens of the same external dimensions for all four groups. Further investigations should be performed on specimens with the same amount of metal because the amount of metal in the cross-section of the SLS-hollow specimen changes with the addition of the hollow structure compared to the other conditions.

5. Conclusions

The following conclusions were obtained after examining the effects of the hollow structure added by SLS on the mechanical properties of Co-Cr alloys:

- SLS-hollow specimens met the ISO 22674 standard for dental metals.
- By adding a hollow structure, the elastic modulus decreased, whereas the mechanical strength and proof stress remained high in SLS specimens.
- No voids were observed in the SLS specimens even with the addition of hollow structures.
- This study suggests that RPD frameworks with high strength and optimal structural properties may be made through SLS.

Acknowledgments

The authors would like to thank the members of the Tokai University Imaging Center for Advanced Research for their assistance and cooperation throughout the study.

Conflict of interest

There are no conflicts of interest to declare regarding this study.

References

[1] Alifui-Segbaya F, Williams RJ, George R. Additive manufacturing: a novel method for fabricating cobalt-chromium removable partial denture frameworks. Eur J Prosthodont Restor Dent. 2017;25:73–8. https://doi.org/10.1922/EJPRD_1598Alifui-Segbaya06, PMID:28590092

[2] Williams RJ, Bibb R, Eggbeer D, Collis J. Use of CAD/CAM technology to fabricate a removable partial denture framework. J Prosthet Dent. 2006;96:96–9. https://doi.org/10.1016/j.prosdent.2006.05.029, PMID:16911885

[3] Ye H, Ning J, Li M, Niu L, Yang J, Sun Y, *et al.* Preliminary clinical application of removable partial denture frameworks fabricated using computer-aided design and rapid prototyping techniques. Int J Prosthodont. 2017;30:348–53. https://doi.org/10.11607/ijp.5270, PMID:28697204

[4] Kim H, Jang SH, Kim Y, Son J, Min B, Kim KH, *et al.* Microstructures and mechanical properties of Co-Cr dental alloys fabricated by three CAD/CAM-based processing techniques. Materials (Basel). 2016;9:596. https://doi.org/10.3390/ma9070596, PMID:28773718

[5] Tasaka A, Kato Y, Odaka K, Matsunaga S, Goto T, Abe S, *et al.* Accuracy of clasps fabricated with three different CAD/CAM technologies: casting, milling, and selective laser sintering. Int J Prosthodont. 2019;32:526–9. https://doi.org/10.11607/ijp.6363, PMID:31664269

[6] Alageel O, Abdallah MN, Alsheghri A, Song J, Caron E, Tamimi F. Removable partial denture alloys processed by laser-sintering technique. J Biomed Mater Res B Appl Biomater. 2018;106:1174–85. https://doi.org/10.1002/jbm.b.33929, PMID:28561993

[7] McCabe JF, Walls AWG. Applied dental materials, 9th ed.Oxford, UK, Blackwell Publishing Ltd; 2008, p. 71–9.

[8] Koutsoukis T, Zinelis S, Eliades G, Al-Wazzan K, Rifaiy MA, Al Jabbari YS. Selective laser melting technique of Co-Cr dental alloys: a review of structure and properties and comparative analysis with other available techniques. J Prosthodont. 2015;24:303–12. https://doi.org/10.1111/jopr.12268, PMID:26129918

[9] Conner BP, Manogharan GP, Martof AN, Rodomsky LM, Rodomsky CM, Jordan DC, *et al.* Making sense of 3-D printing: creating a map of additive manufacturing products and services. Addit Manuf. 2014;1-4:64–76. https://doi.org/10.1016/j.addma.2014.08.005

[10] Thompson MK, Moroni G, Vaneker T, Fadel G, Campbell RI, Gibson I, *et al.* Design for Additive Manufacturing: Trends, opportunities, considerations, and constraints. CIRP Ann. 2016;65:737–60. https://doi.org/10.1016/j.cirp.2016.05.004

[11] Milewski JO. Additive manufacturing of metals: from fundamental technology to rocket nozzles, medical implants, and custom jewelry. Springer; 2017, p.7-33. https://doi.org/10.1007/978-3-319-58205-4.

[12] Yang L, Hsu K, Baughman B, Godfrey D, Medina F, Menon M, *et al.* Additive manufacturing of metals: the technology, materials, design and production.Springer; 2017. https://doi.org/10.1007/978-3-319-55128-9.

[13] Remouchamps A, Bruyneel M, Fleury C, Grihon S. Application of a bi-level scheme including topology optimization to the design of an aircraft pylon. Struct Multidiscipl Optim. 2011;44:739–50. https://doi.org/10.1007/s00158-011-0682-3

[14] Wohlers T, Campbell I, Diegel O, Huff R, Kowen J. 3D printing and additive manufacturing state of the industry: annual worldwide progress report. Lund, Sweden, Lund University; 2017.

[15] Bartolomeu F, Dourado N, Pereira F, Alves N, Miranda G, Silva FS. Additive manufactured porous biomaterials targeting orthopedic implants: A suitable combination of mechanical, physical and topological properties. Mater Sci Eng C. 2020;107:110342. https://doi.org/10.1016/j.msec.2019.110342, PMID:31761155

[16] Morris HF, Asgar K, Tillitson E. Stress-relaxation testing. Part I: A new approach to the testing of removable partial denture alloys, wrought wires, and clasp behavior. J Prosthet Dent. 1981;46:133–41. https://doi.org/10.1016/0022-3913(81)90294-8, PMID:6944476

[17] Stade EH, Stewart GP, Morris HF, Pesavento JR. Influence of fabrication technique on wrought wire clasp flexibility. J Prosthet Dent. 1985;54:538–43. https://doi.org/10.1016/0022-3913(85)90430-5, PMID:3900348

[18] Hindels GW. Stress analysis in distal extension partial dentures. J Prosthet Dent. 1957;7:197–205. https://doi.org/10.1016/0022-3913(57)90075-6

[19] Kim SY, Shin SY, Lee JH. Effect of cyclic bend loading on a cobalt-chromium clasp fabricated by direct metal laser sintering. J Prosthet Dent. 2018;119:1027. e1-1027. e7. https://doi.org/10.1016/0022-3913(57)90075-6, PMID:29980268

[20] Carr AB, Brown DT. McCracken's removable partial prosthodontics, 12th ed. Elsevier St. Louis; 2010, p.67-95.

[21] Tsolka P, Altay OT, Preiskel HW. Effect of the major connector on abutment tooth and denture base movement: an in vitro study. Int J Prosthodont. 1990;3:545–9. PMID:2083023

[22] Barbenel JC. Design of partial denture components. I. Middle palatal bars. J Dent Res. 1971;50:586–9. https://doi.org/10.1177/00220345710500031001, PMID:4930311

[23] Ben-Ur Z, Matalon S, Aviv I, Cardash HS. Rigidity of major connectors when subjected to bending and torsion forces. J Prosthet Dent. 1989;62:557–62. https://doi.org/10.1016/0022-3913(89)90079-6, PMID:2691659

[24] Carr AB, Brown DT. McCracken's removable partial prosthodontics, 12th ed. Elsevier St. Louis; 2010, p. 29-55.

[25] Phoenix RD, Cagna DR, Defreest CF. Stewart`s clinical removable partial prosthodontics, fourth ed. Quintessence; 2008, p.51-83.

[26] Kaires AK. Effect of partial denture design on bilateral force distribution. J Prosthet Dent. 1956;6:373–85. https://doi.org/10.1016/0022-3913(56)90058-0

[27] Henderson D, Seward TE. Design and force distribution with removable partial dentures: A progress report. J Prosthet Dent. 1967;17:350–64. https://doi.org/10.1016/0022-3913(67)90006-6, PMID:5230384

[28] Phoenix RD, Cagna DR, Defreest CF. Stewart`s clinical removable partial prosthodontics, fourth ed. Quintessence; 2008, p. 19-36.

[29] Schweiger J, Güth JF, Erdelt KJ, Edelhoff D, Schubert O. Internal porosities, retentive force, and survival of cobalt–chromium alloy clasps fabricated by selective laser-sintering. J Prosthodont Res. 2020;64:210–6. https://doi.org/10.1016/j.jpor.2019.07.006, PMID:31680054

[30] Tasaka A, Shimizu T, Kato Y, Okano H, Ida Y, Higuchi S, *et al.* Accuracy of removable partial denture framework fabricated by casting with a 3D printed pattern and selective laser sintering. J Prosthodont Res. 2020;64:224–30. https://doi.org/10.1016/j.jpor.2019.07.009, PMID:31466919

[31] Chen H, Li H, Zhao Y, Zhang X, Wang Y, Lyu P. Adaptation of removable partial denture frameworks fabricated by selective laser melting. J Prosthet Dent. 2019;122:316–24. https://doi.org/10.1016/j.prosdent.2018.11.010, PMID:30922559

[32] ISO 22674:2016 Dentistry—metallic materials for fixed and removable restorations and appliances; international organization for standardization: Geneva, Switzerland, 2016.

[33] Rasband WS, Image JUS. National institutes of health, Bethesda, Maryland, USA, http://rsb.info.nih.gov/ij/, 1997-2012.

[34] Schneider CA, Rasband WS, Eliceiri KW. NIH Image to ImageJ: 25 years of image analysis. Nat Methods. 2012;9:671–5. https://doi.org/10.1038/nmeth.2089, PMID:22930834

[35] Abramoff MD, Magelhães PJ, Ram SJ. Image processing with ImageJ. Biophoton Int. 2003;11:36–42.

[36] Ikeo N, Ishimoto T, Nakano T. Novel powder/solid composites possessing low Young's modulus and tunable energy absorption capacity, fabricated by electron beam melting, for biomedical applications. J Alloys Compd. 2015;639:336–40. https://doi.org/10.1016/j.jallcom.2015.03.141

[37] Barro Ó, Arias-González F, Lusquiños F, Comesaña R, del Val J, Riveiro A, *et al.* Effect of four manufacturing techniques (casting, laser directed energy deposition, milling and selective laser melting) on microstructural, mechanical and electrochemical properties of Co-Cr dental alloys, before and after PFM firing process. Metals (Basel). 2020;10:1291–313. https://doi.org/10.3390/met10101291

[38] Leinfelder KF, Lemons JE. Clinical restorative materials and techniques. Philadelphia: Lea& Febiger; 1988, p. 251-71

[39] Anusavice KJ, Shen C, Rawls HR. Phillips` science of dental materials, 12th ed. Elsevier; 2013, p. 194-230

[40] Mori M, Yamanaka K, Chiba A. Phase decomposition in biomedical Co–29Cr–6Mo–0.2N alloy during isothermal heat treatment at 1073K. J Alloys Compd. 2014;590:411–6. https://doi.org/10.1016/j.jallcom.2013.12.126

[41] Yamanaka K, Mori M, Chiba A. Nanoarchitectured Co–Cr–Mo orthopedic implant alloys: nitrogen-enhanced nanostructural evolution and its effect on phase stability. Acta Biomater. 2013;9:6259–67. https://doi.org/10.1016/j.actbio.2012.12.013, PMID:23253619

[42] Kurosu S, Matsumoto H, Chiba A. Isothermal phase transformation in biomedical Co-29Cr-6Mo alloy without addition of carbon or nitrogen. Metal Mater Trans A. 2010;41:2613–25. https://doi.org/10.1007/s11661-010-0273-8

[43] Lewis AJ. Radiographic evaluation of porosities in removable partial denture castings. J Prosthet Dent. 1978;39:278–81. https://doi.org/10.1016/S0022-3913(78)80095-X, PMID:273090

[44] Karpuschewski B, Pieper HJ, Krause M, Döring J. CoCr is not the same: CoCr-blanks for dental machining. Future Trends Prod Eng. Berlin, Springer-Verlag; 2013, p. 261-74. https://doi.org/10.1007/978-3-642-24491-9_26.

[45] Han X, Sawada T, Schille C, Schweizer E, Scheideler L, Geis-Gerstorfer J, *et al.* Comparative analysis of mechanical properties and metal-ceramic bond strength of Co-Cr dental alloy fabricated by different manufacturing processes. Materials (Basel). 2018;11:1801. https://doi.org/10.3390/ma11101801, PMID:30249000

[46] Prashanth KG, Scudino S, Klauss HJ, Surreddi KB, Löber L, Wang Z, *et al.* Microstructure and mechanical properties of Al–12Si produced by selective laser melting: effect of heat treatment. Mater Sci Eng A. 2014;590:153–60. https://doi.org/10.1016/j.msea.2013.10.023

[47] Xin X-Z, Chen J, Xiang N, Gong Y, Wei B. Surface characteristics and corrosion properties of selective laser melted Co–Cr dental alloy after porcelain firing. Dent Mater. 2014;30:263–70. https://doi.org/10.1016/j.dental.2013.11.013, PMID:24388219

[48] Zhou Y, Li N, Yan J, Zeng Q. Comparative analysis of the microstructures and mechanical properties of Co-Cr dental alloys fabricated by different methods. J Prosthet Dent. 2018;120:617–23. https://doi.org/10.1016/j.prosdent.2017.11.015, PMID:29627206